We are IntechOpen,
the world's leading publisher of
Open Access books
Built by scientists, for scientists

6,900
Open access books available

185,000
International authors and editors

200M
Downloads

154
Countries delivered to

Our authors are among the

TOP 1%
most cited scientists

12.2%
Contributors from top 500 universities

BOOK CITATION INDEX INDEXED
CLARIVATE ANALYTICS

WEB OF SCIENCE™

Selection of our books indexed in the Book Citation Index
in Web of Science™ Core Collection (BKCI)

Interested in publishing with us?
Contact book.department@intechopen.com

Numbers displayed above are based on latest data collected.
For more information visit www.intechopen.com

Pyrimidinylsalicylic Based Herbicides: Modeling and Prediction

Eduardo J. Delgado
Theoretical and Computational Chemistry Group (QTC)
Department of Physical-Chemistry, Faculty of Chemical Sciences
Universidad de Concepción, Concepción,
Chile

1. Introduction

The necessity of increasing the productivity per cultivation area is a peremptory demand since, on hand, the available surface is limited, even worse it has diminished due to the degradation of the soil; and on the other hand, it is necessary to supply the food demand of a steadily increasing population.

To supply this demand of the current world population, about six thousand million, it is required to produce more and more. To do this is necessary to use massively chemicals, known generically as agrochemicals (insecticides, fungicides, acaricides, nematocides and herbicides). The use of these chemicals has allowed for significant reduction of the agriculture plagues and consequently increased the productivity. Among the pesticides, the herbicides deserve special attention since, due to the resistance developed by weeds, new products have to be steadily introduced to market.

Plants and many microorganisms are able to synthesize from inorganic precursors all the metabolites needed for their survival. In contrast, animals must obtain many compounds, such as vitamins, essential fatty acids and certain amino acids, from their diet. This is because they lack the full biosynthetic machinery, so there are metabolic pathways and their component enzymes that are not found in animals. The branched-chain amino acids (BCAAs) are synthesized by plants, algae, fungi, bacteria and archae, but no by animals. Therefore, the enzymes involved in the BCAA biosynthetic pathway are potential targets for the development of herbicides, fungicides, and antimicrobial compounds.

Pyrimidinylsalicylic acid (PSA) based compounds show potent herbicidal activity. This activity has been identified as a result of the inhibition of acetohydroxyacid synthase, AHAS. Unfortunately, this family of compounds has been poorly characterized from the physical-chemical point of view. This lack of information has prevented the assessment of their impact in the environment. The difficulty to obtain accurate experimental values arise mainly from limitations of analytical techniques, cost, safety and time. For this reason, it is very useful to be able to predict these properties. Such a prediction may be important additionally for the design of novel herbicides since their properties could be predicted prior to synthesis and consequently the design may, in this way, be guided by the results of calculations. Once these properties are known the effect of these chemicals on the environment could be evaluated in advance, reaching in this way the desired compromise

between productivity and environment protection. In this chapter, classical and quantum chemical methods are applied to predict and calculate important properties of PSA based herbicides.

2. Partitioning of a chemical in the environment

When a chemical is released in the environment it distributes among the diverse compartments which comprise it, Figure 1, (Stangroom et al., 2000; Ballschmiter, 1992). A knowledge of chemical partitioning is needed to assess pathways of pollutant transport and transformation. Hence, a detailed understanding of chemical partitioning behaviour is a fundamental requirement for the development of environment models for the assessment of contaminant fate. An improved understanding of chemical partitioning would facilitate the estimation of exposure levels in the various environment compartments (soil, water, air and biota). Being the acid dissociation constant pK_a one of the most important of such parameters because ionization alters the macro properties such as solubility and lipophilicity.
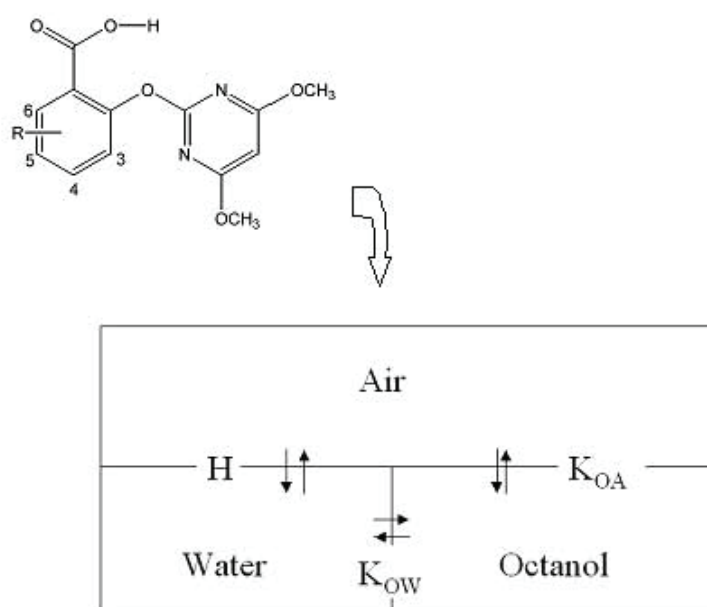

Fig. 1. Distribution of PSA compounds in the environment.

3. Pyrimidinyl salicylic acids

The synthesis and herbicidal activity of pyrimidinylsalicylic acid (PSA) based compounds, Figure 2, was reported for first time by Nezu et al. (Nezu et al., 1996; Nezu et al., 1998). These compounds show highly potent herbicidal activity characteristic of AHAS inhibition. The effect of substituents R introduced into various positions of the benzene ring is striking. Some substituents at the 6-position increase the AHAS inhibitory activity enormously, whereas others, as well as most substituents at the other positions, have the reverse effect. The replacement of O, in the X position, with S does not much affect the AHAS inhibition except for a few pairs of analogs. The phytotoxicity in the oxy-series is, however, reduced, in general, in the corresponding thio-series. The extent of the toxicity reduction varies depending on the crop/weed species, leading to selectively herbicidal thiosalicylic acids.
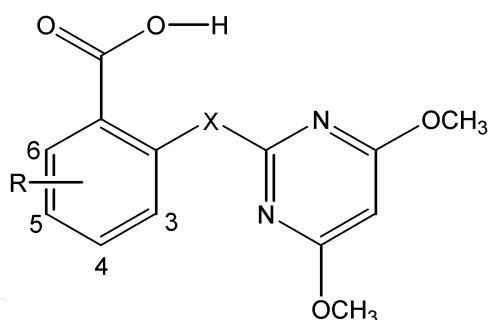
Fig. 2. General structure of PSA compounds: X=O, S

4. Acetohydroxyacid synthase.

Acetohydroxyacid synthase, AHAS, the first common enzyme in the biosynthetic route to the branched chain amino acids, valine, leucine and isoleucine, Figure 3, has been identified as the target of action of several structurally different types of chemicals (sulfonylureas, sulfonamides, imidazolinones and pyrimidylsalicylates) with high herbicidal activity. These four classes of herbicides, all obtained by traditional screening methods, have the attributes of low application rates, good crop selectivity, environmental safety and low mammalian toxicity. These herbicides act inhibiting AHAS leading to the starvation of the plant for these amino acids, it is this starvation that is thought to be the primary mechanism by which these chemicals cause plant death (Singh & Shaner, 1995; Zohar et al., 2003; Pang et al., 2002, Pang et al., 2003; McCourt et al., 2005; MCCourt et al., 2006; Duggleby & Pang, 2000; MCCourt & Duggleby, 2006).
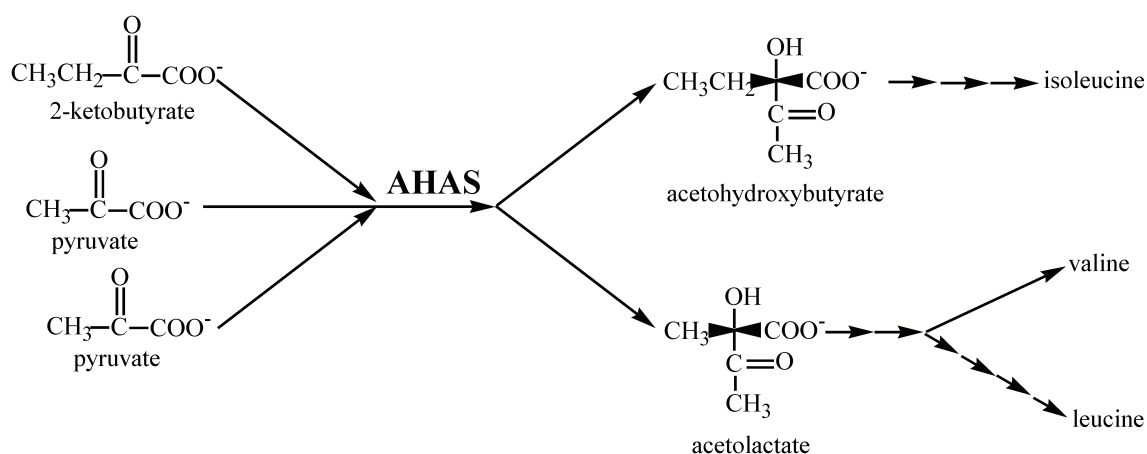

Fig. 3. Branched-chain amino acid biosynthesis pathway

Valine, leucine and isoleucine are synthesized by a common pathway in micro organisms and plants. One unusual feature of this pathway is the employment of parallel steps leading to the formation of valine and isoleucine. These parallel steps involve four enzymes, namely the anabolic AHAS, ketol-acid reductoisomerase, dihydroxyacid dehydratase, and a transaminase, each of which is capable of catalyzing two slightly different reactions.

The anabolic AHAS catalyzes the first of the parallel steps and is at branch point in the pathway because its reactions will determine the extent of carbon flow through to the branched-chain amino acids. The reactions involve the irreversible decarboxylation of pyruvate and the condensation of the acetaldehyde moiety with a second molecule of

pyruvate to give 2-acetolactate or with a molecule of 2-ketobutyrate to yield 2-aceto-2-hydroxybutyrate.

Each of the products in then converted further in three reactions to give valine and isoleucine; for leucine biosynthesis, four additional enzymes are required using valine precursor 2-ketoisovalerate as the starting point for synthesis.

The regulation of the biosynthesis of the branched–chain amino acids is complex and carefully controlled. This regulation is essential, not only to ensure a balanced supply of the amino acids within cells, but also because its intermediates interact with other cellular metabolic pathway. Even through microbes and plants share the common branched-chain amino acid pathway, its regulation may vary among organisms and is not fully understood.

AHAS belongs to a super family of thiamine diphosphate, ThDP, dependent enzymes that are capable of catalyzing a variety of rections, including both the oxidative and non-oxidative decarboxylation of 2-ketoacids. This cofactor is bound by a divalent metal ion such as Mg^{+2}, which coordinates to the diphosphate group of ThDP and two highly conserved residues in these proteins (Mc Court et al., 2006). AHAS also binds a molecule of flavin adenine dinucleotide, FAD. There is no intrinsic feature of the reaction catalyzed that demands this requirement, and is demonstrated by the fact that there is an FAD-independent form of the enzyme in some bacteria. The hypothesis that FAD plays a purely structural role is supported by comparison of the structures of the FAD-dependent and FAD-independent enzyme (Pang et al., 2004).

5. Molecular approaches to studying chemistry in solution.

Modern chemistry is oriented more and more towards elucidating in detail how the macroscopic properties are determined by the microscopic properties of matter, thus enabling subsequent experimentation to be concentrated in the most promising directions. There exist several approaches for the prediction of chemical properties in solution, which may be classified as: discrete, classical and quantum chemical methods.

Discrete methods based on statistical mechanics, link those two pictures through the probabilistic treatment of particle ensembles. The most popular are molecular dynamics (MD) and the Monte Carlo (MC) method. In both cases, the condensed system is represented by an assembly of interacting particles, the statistical distribution of any property, or its evolution in time, is obtained as a sum over all particles, with appropriate rules. Applications of such techniques to study phase equilibria have been reported widely in literature (Frenkel & Smit, 1996; Siepmann, 1999; Duffy & Jorgensen, 2000; Kollman, 1993). Although some simple hydrocarbons can nowadays be reasonably well described by MD and MC methods, water and especially water mixtures, still represent challenges for such simulations techniques despite 30 years of active parameterization of appropriate force-fields. This is due to the extremely strong and complicated electrostatic and hydrogen-bonding interactions (Estrada et al., 2007).

The best developed classical method is the multivariate quantitative structure-activity/property relationship (QSAR/QSPR) methodology (Katritzky at al., 1997; Karelson et al., 1996; Hansch at al., 1996; Hansch, 1993, Cramer at al., 1988; Klebe at al., 1994). The underlying assumption in this methodology is that the molecular structure of an organic compound contains, in principle, coded within it all of the information which predetermines the chemical, biological and physical properties of that compound. If we could elucidate in detail how these properties are determined by structure, we could predict such properties

simply from a knowledge of the molecular structure. A major goal of a QSAR/QSPR study is to find a mathematical relationship between a certain property and one or more descriptive parameters, known as descriptors, related to the structure of the molecule. These descriptors are numerical representations of structural features of molecules that attempt to encode important information that causes structurally different compounds to have different property values. These models so developed are important for the design of novel compounds since properties can be predicted prior to synthesis, and in this way the design of new chemicals, with specific properties, may be guided by the calculation results.

Quantum mechanical continuum solvation methods (Tomasi & Persico, 1994; Cramer, 2002; Young, 2001) are based on the self-consistent reaction field (SCRF) approach which considers the solvent as a structureless and continuous dielectric medium, characterized with a dielectric constant ε, with the solute placed in a suitable shaped hole within it. The SCRF method is an adaptation of the Poisson method for *ab initio* calculations. There are quite a number of variations on this method. One point of difference is the shape of the solvent cavity. Various models use spherical cavities, spheres for each atom, or an isosurface of electron density. The second difference is the description of the solute, which could be a dipole, multipole expansion, or numerical integration over the charge density.

The quantum mechanical based methods have been developed to the point that they are useful tools for predicting thermodynamic properties and phase behaviour of some substances to an accuracy useful in engineering calculations (Sandler, 2003).

6. Prediction of PSA properties: three case studies

6.1 Quantitative prediction of AHAS inhibition by PSA compounds

We have studied AHAS inhibition by PSA based herbicides within the framework of quantitative structure-activity relationship (QSAR) methodology (Diaz & Delgado, 2009). A general model for this family of herbicides has been developed to predict molar pI_{50}, i.e, the logarithm of the reciprocal molar concentration of herbicide required for 50% inhibition of the AHAS activity. The model involves only four descriptors: two geometric and two quantum chemical, accounting for the steric, electrostatic and hydrogen bonding interactions responsible for the binding of the herbicide to the enzyme.

6.1.1 Chemical data

The data set of the pI_{50} was taken from the data reported by Nezu *et al.* (1998). The set contains 46 structures of substituted *O*-(4,6-dimethoxypyrimidin-2-yl)salicylic acids and thio analogs inhibiting AHAS, including 6-substituted(thio)-, 5- and 6- substituted salicylic acids; covering a pI_{50} range from about 3 to 8 units.

6.1.2 Methodology

Empirical evidences show that the acidic carboxyl group of these pyrimidylsalicylates is indispensable for AHAS inhibition; moreover, it has been suggested the carboxylate group is responsible for the binding of the inhibitor molecule to the enzyme (Nezu at al., 1998). Enzymes are proteins which are actives under relative mild reactions conditions: temperature below 100^0C, atmospheric pressure and nearly neutral pH. Therefore, at these conditions of pH the PSA compounds will be in their anionic form, since their pK_a values go from about 3.3 to 4.4 (Delgado, 2009).

Modeling was performed in order to set the anions in their lowest energy 3D conformations. To achieve this goal, initial three-dimensional geometries of the chemical structures were generated using Hyperchem 7.0 molecular modeling package. These 3D structures were refined later using Ampac 5.0, a semiempirical molecular modeling program, using AM1 parameterization. To determine the lowest-energy conformations for each molecule, geometry optimizations were carried out allowing one or more torsional angles to vary systematically. The keyword CHARGE= -1 was always used in all cases. The Ampac output files, containing the lowest–energy structures and the respective electron wave functions of individual compounds, were loaded into the Codessa program to calculate the molecular descriptors. This pool of descriptors was reduced by removing descriptors that could not be calculated for every structure in the data set, and by eliminating one descriptor from those pairs highly correlated. Afterwards, from this reduced pool of descriptors the best multilinear correlation QSAR model was searched using the Sigmastat statistical package

6.1.3 Results

A total of 184 descriptors, 12 geometrical and 172 quantum chemical, were calculated for all compounds. The best regression equation found involves only four descriptors, two geometrical and two quantum chemical: S_M, the molecular surface area; S_{XY}, the normalized shadow area of the molecule projected on the XY plane; HOMO, the energy of the highest occupied molecular orbital; and FNSA, the fractional partial negatively charged surface area. It is noteworthy that these descriptors individually correlate poorly with the property (R^2 = 0.22, 0.27, 0.11, 0.01 for S_M, S_{XY}, HOMO and FNSA, respectively), however they collectively correlate pretty well with the property, R^2 = 0.89. This is an interesting result since, from the respective individual correlation coefficient, these descriptors are seemingly not relevant for predicting inhibition. Nevertheless, the relevance of these descriptors it is made evident only when the correlation with the collective is considered. This means that the interaction of information among the descriptors add an important additional predictive value which goes further from the simple sum of the information contained in the individual descriptors. This finding is in agreement with the widely accepted idea that inhibition is driven by several interactions (steric, electrostatic and hydrogen-bonding) which occur simultaneously and synergically. The best regression equation found is the following:

$$pI_{50} = 13.70 - 0.04\,S_M + 18.77\,S_{XY} + 0.79\,HOMO - 4.99\,FNSA \qquad (1)$$

and its respective statistics is shown in Tables 1 and 2.

In these tables the statistical parameters have the usual meaning. The p-values indicate that all descriptors are statistically significant at the 99% confidence level. On the other hand, the VIF values, about 1, indicate there is no serious collinearity between the involved descriptors (Ott & Longnecker, 2001). Therefore, it is concluded that all the independent variables included in the model are relevant.

The experimental and calculated values of pI_{50} along with the values of the descriptors involved in the model are shown in Table 3. The respective scatter plot is shown in Figure 4. To check the predictive capability of the model, it was tested with an external set of chemicals not contains in the training set. The validation data set included 13 chemicals

including 5- and 6- substituted salicylic acids as well as 6- substituted thio analogs. In Table 4, the values of the molecular descriptors along with the experimental and calculated values of pI_{50} for the validation set are shown. The statistics for the validation is as follows: $R^2 = 0.84$, s = 0.33, F= 59. These results confirm the prediction capability of the model.

	Coefficient	Std. Error	p-value	VIF
Constant	13.70	2.76	< 0.001	
S_M	-0.04	0.003	< 0.001	1.31
S_{XY}	18.77	2.39	< 0.001	1.81
HOMO	0.79	0.26	0.006	1.99
FNSA[1]	-4.99	1.30	< 0.001	1.11
$R^2 = 0.89$, $R^2_{CV} = 0.85$, $R^2_{df} = 0.88$, s = 0.43				

Table 1. Statistical parameters for the best QSAR model

Analysis of Variance				
	DF	SS	MS	F	P
Regression	4	37.38	9.34	52	< 0.001
Residual	25	4.53	0.18		
Total	29	41.91	1.44		

Table 2. Analysis of variance of the best QSAR model
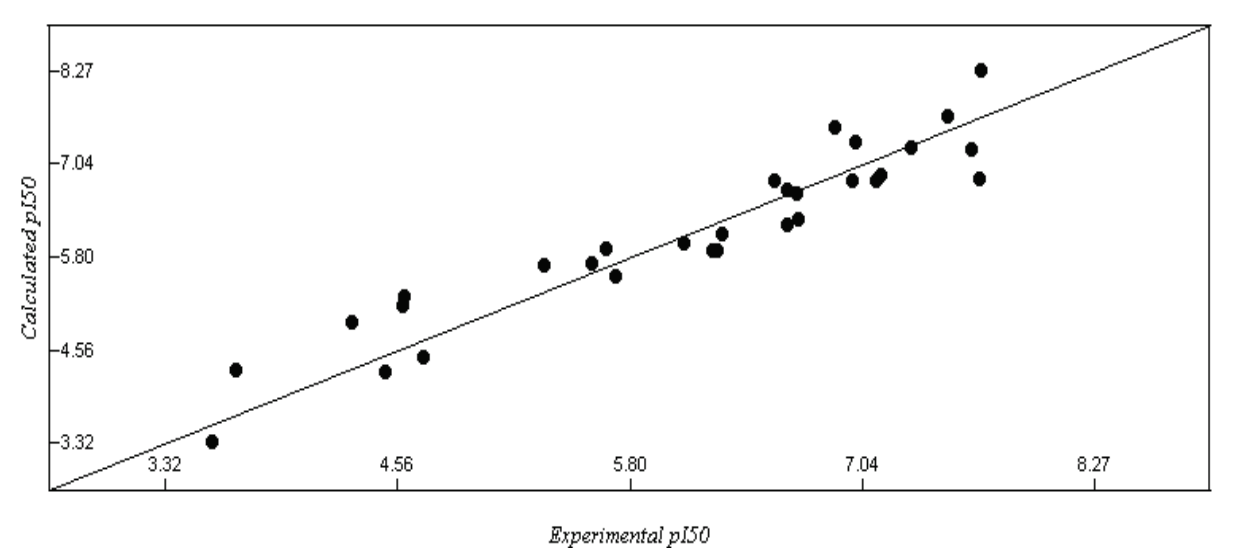
Fig. 4. Scatter plot of the calculated vs. experimental pI_{50}

Y	S_M	S_{XY}	HOMO	FNSA[1]	pI_{50} (exp)	pI_{50} (calc)	Diff.
5-substituted Pyrimidinylsalicilates							
F	279.23	0.57	-5.35	0.47	6.27	5.86	-0.41
Cl	313.83	0.63	-4.92	0.53	5.35	5.67	0.32
Br	318.11	0.57	-4.93	0.54	4.50	4.25	-0.25
C_2H_5	310.27	0.56	-5.17	0.35	4.59	5.15	0.56
OCH_3	300.19	0.55	-5.21	0.39	4.60	5.25	0.65
OC_6H_5	357.88	0.60	-5.40	0.42	3.58	3.32	-0.26
SCH_3	338.00	0.61	-4.86	0.38	4.32	4.93	0.61
CN	301.27	0.56	-5.51	0.53	3.71	4.29	0.58
NH_2	285.19	0.57	-5.17	0.42	6.09	5.98	-0.11
CCH	309.95	0.57	-5.28	0.50	4.70	4.45	-0.25
6-substituted Pyrimidinylsalicilates							
H	268.10	0.57	-5.16	0.42	6.64	6.69	0.05
F	267.34	0.61	-5.24	0.46	7.30	7.23	-0.07
Cl	273.62	0.63	-5.18	0.50	7.62	7.21	-0.41
I	281.59	0.60	-5.21	0.40	7.66	6.83	-0.83
CH_3	280.47	0.62	-5.13	0.38	6.89	7.51	0.62
C_2H_5	294.75	0.62	-5.12	0.37	6.57	6.81	0.24
OC_3H_7	309.91	0.60	-5.25	0.33	6.24	5.87	-0.37
$OCH(CH_3)_2$	322.80	0.62	-5.22	0.37	5.73	5.54	-0.19
SC_2H_5	316.95	0.62	-4.31	0.33	7.11	6.79	-0.32
SC_3H_7	324.40	0.60	-4.32	0.32	6.29	6.10	-0.19
NO_2	292.87	0.63	-5.65	0.48	6.64	6.21	-0.43
CO_2CH_3	307.35	0.62	-5.56	0.41	5.68	5.89	0.21
NH_2	280.47	0.62	-5.24	0.39	7.00	7.32	0.32
6-substituted Pyrimidinyl(thio)salicylates							
F	301.31	0.70	-4.35	0.47	7.67	8.27	0.60
Cl	308.83	0.69	-4.32	0.49	7.49	7.65	0.16
I	294.59	0.62	-5.11	0.39	6.99	6.80	-0.19
OC_2H_5	341.24	0.65	-4.19	0.36	6.70	6.30	-0.40
OC_6H_5	364.64	0.70	-4.37	0.44	5.60	5.69	0.09
NO_2	324.48	0.69	-4.71	0.51	6.69	6.63	-0.06
$COCH_3$	326.72	0.68	-4.43	0.44	7.14	6.87	-0.27

Table 3. Molecular descriptors and values of experimental and calculated pI_{50} for the training set.

Y	S_M	S_{XY}	HOMO	FNSA[1]	pI_{50} (exp)	pI_{50} (calc)	Diff.
5-substituted Pyrimidinylsalicilates							
H	268.10	0.57	-5.16	0.42	6.64	6.69	0.05
I	321.03	0.55	-4.93	0.39	5.05	4.50	-0.55
OH	308.43	0.69	-4.87	0.48	7.20	7.29	0.09
6-substituted Pyrimidinylsalicylates							
C_3H_7	310.23	0.61	-5.15	0.35	5.89	6.17	0.28
OC_2H_5	302.35	0.66	-5.22	0.33	7.05	7.37	0.32
OC_4H_9	328.96	0.64	-5.15	0.32	6.21	5.98	-0.23
CF_3	289.31	0.68	-5.51	0.52	6.96	7.15	0.19
6-substituted Pyrimidinyl(thio)salicylates							
Br	288.99	0.63	-5.08	0.40	7.40	7.23	-0.17
CH_3	286.51	0.67	-4.98	0.41	7.53	8.05	0.52
OCH_3	323.96	0.67	-4.20	0.39	7.05	7.18	0.13
SC_2H_5	345.36	0.65	-4.26	0.35	6.67	6.13	-0.54
CF_3	326.52	0.69	-4.52	0.55	6.02	6.48	0.46
COC_6H_5	366.52	0.72	-4.46	0.45	5.19	5.75	0.56

Table 4. Molecular descriptors and values of experimental and calculated pI_{50} for the validation set.

6.1.4 Discussion

From the explanations suggested in literature, it seems to be logical to think the first requirement that the inhibitors must meet is the steric factor, since the chemicals must fit in the active site channel. To this the chemical has to have the adequate size and the shape. Consequently, the more relevant descriptors in the model are the molecular surface area and the shadow area of the molecule projected on the XY plane. These descriptors encode the size and the geometrical shape of the molecule, respectively. The normalized shadow indices, introduced by Jurs as molecular shape descriptors (Stanton & Jurs, 1990), are calculated as the ratio of the areas of three orthogonal projections to the maximum dimensions along the respective axes, taking the X coordinate along the main axis of inertia and so on.

The correlation coefficients for the above two descriptors have opposite sign, indicating size and shape have antagonistic effects on inhibition. Thus, on one hand, the pI_{50} value decreases as the surface area increases; on the other hand, the normalized shadow area in the XY plane, S_{XY}, increases the value of pI_{50}. Therefore, both descriptors have inverse effect on inhibition, disfavoring and favoring inhibition, respectively. This inverse effect is presumably due to the inhibitors must accommodate in a size-limited cavity in the enzyme, on one hand; and to enter into the enzyme the inhibitors should have the adequate conformation to facilitate the entry and to favor the diverse intermolecular interaction with amino acid side chains, on the other hand. The conformations which maximize the shadow XY area are those in which the benzene ring and the pyrimidinyl ring are aligned in the

same plane in such a way the main moment of inertia lies in this plane. This conformation, which is observed in the thio-derivates, facilitates the entry of the inhibitor into the active site channel and set the ring atoms in a favorable position to make interactions with the amino acids side chains. In the other two families instead the benzene and the pyrimidinyl ring lies in planes almost orthogonals each other, adopting a nearly L-shaped structure hindering the entry into the active site tunnel.

The correlation coefficient for the HOMO energy is positive indicating the property, pI_{50}, and this descriptor vary in symmetrical way, i.e., the higher the value of the Homo energy the higher the value of pI_{50}, which means a lower molar concentration for 50% inhibition of the enzyme activity. Therefore, the HOMO energy is a key descriptor for an increased inhibitory potency. The energy of the HOMO characterizes the susceptibility of the molecule toward attack by electrophiles. Thus, it is expected this descriptor is involved in hydrogen bonding interactions between partners with complementary properties, i.e. hydrogen acceptors on the ligand and hydrogen donors on the receptor. It has been well established that this type of interaction is one of the factors responsible for the binding of the inhibitor to the enzyme. The carboxylate group is expected to be the key for the extent of these interactions due to its ability to act as hydrogen acceptor because of the high electron density on the oxygen atoms of this group. This could explain the empirical finding about the carboxylate group is indispensable for AHAS inhibition because of its crucial role in the binding of the inhibitor to the enzyme.

The fourth descriptor in relevance is the fractional partial negatively charged surface area, $FNSA^{(1)}$, i.e. the ratio of the partial negatively charged surface area to the total molecular surface area (Stanton & Jurs, 1990); encoding features related to polar interactions. Its respective correlation coefficient is negative indicating this electrostatic factor disfavors the inhibition. This effect is similar to that observed in the inhibition of AHAS by sulfonylurea herbicides (Wang at al., 2005), wherein the chemicals need contributions from positively charged groups to achieve enhanced inhibition, and only small areas of the active site channel of AHAS have preference for negatively charged groups. This analog trend between these two families of herbicides seems to suggest they share the same binding site in the enzyme or partially overlapping sites. This finding has already been observed for imidazolinones, as well. These results are in agreement with recently reported results obtained by the integration of molecular docking, CoMFA, CoMSIA and DFT calculations (He at al., 2007). Nevertheless, our model predicts pI_{50} with fewer descriptors and similar statistics than those models reported in the just mentioned article. In QSAR modeling, the Parsimony Principle (Occam´s Razor Principle) calls for using models and procedures that contain all that is necessary for the modeling but nothing more, i.e. given a number of models with nearly the same predictive error, that containing fewer parameters should be preferred because simplicity is desirable in itself (Estrada et al., 2004).
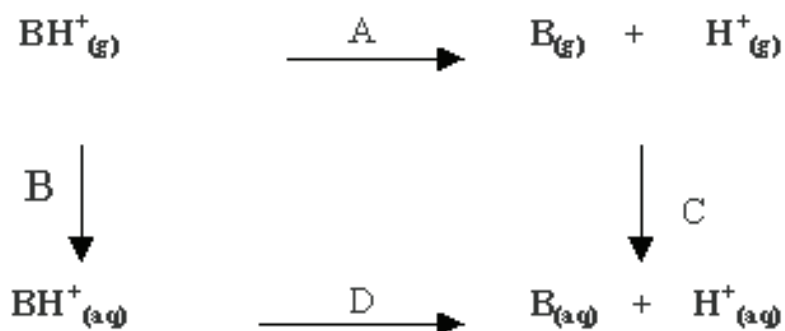
6.2 DFT calculation of pK_a´s for PSA based herbicides

The acid-dissociation constant, pK_a, of a compound influences many characteristics of the compound such as its reactivity. In biochemistry, the pK_a values of pesticides are of major importance for the activity of the related enzymes. In environment chemistry, this property is of general importance because ionization of a compound alters its physical behavior and macro properties such as solubility and lipophilicity. The nature and location of substituents may induce drastic changes in the values of the acid-dissociation constants, and consequently important changes in the physical and chemical properties. The interest in determine the

pKa values of diversely substituted chemicals is, on one hand, to correlate the substituent effect and the observed pKa value; and, on the other hand, to evaluate its effect on derived physical-chemical properties. We have calculated the acid-dissociation constants for 39 PSA derived herbicides by using density functional theory (DFT) methods at B3LYP/6-31G(d,p) level of theory (Delgado, 2009).

6.2.1 Computational methods

The quantum chemical calculations were carried out using Jaguar and its graphic interface Maestro. Gas-phase molecular geometries and electronic energies were computed at DFT B3LYP/6-31G(d,p) level of theory. To determine the lowest-energy conformations for each molecule, geometry optimizations were carried out allowing one or more torsional angles to vary systematically. Free energies of solvation in water were computed by single point calculation on the gas-phase optimized geometry using the Poisson-Boltzmann Solvation Model (PB) (Marten at al., 1996). The pKa values were calculated with the Jaguar pKa prediction module using the following thermodynamic cycle, scheme 1, and subsequent equation:

$$BH^+_{(g)} \xrightarrow{\quad A \quad} B_{(g)} + H^+_{(g)}$$

$$\downarrow B \qquad\qquad\qquad \downarrow C$$

$$BH^+_{(aq)} \xrightarrow{\quad D \quad} B_{(aq)} + H^+_{(aq)}$$

Scheme 1. Thermodynamic cycle used to calculate the pKa.

$$pK_a = \frac{1}{2.3\,RT} D \tag{2}$$

where D is the free energy change involved in the step D, and may be calculated from the free energy changes of the other cycle steps by the following relation: D = A+ C - B. In this cycle, the BH+ species refers to the adduct formed from the reaction between the electron-pair donor B species, Lewis base, and the electron-pair acceptor H+ species, Lewis acid.

6.2.2 Results and discussion

The calculated values of pKa's, Table 5, fall in a very narrow range going from 3.3 to 4.4, as it was conjectured by Nezu et al. (1998). However, small differences in the pKa scale may entail large changes in the degree of ionization and related properties such as enzyme inhibition and environmental fate. Therefore, the knowledge of the pKa for each compound, rather than to take an average value for the all family, is of fundamental importance to get a better comprehension of the behavior of these compounds since the average value does not account for the differences observed in the properties of different substituted compounds. Unfortunately, as mentioned above, for these compounds there is no experimental pKa data available to validate the calculated figures. However, considering that the observed

differences in the values of the pK$_a$'s have to be effect of the R-substituent group, since the O-dimethoxypyrimidynil (ODMP) group keeps constant for all compounds, an estimation of the reliability of the calculated figures can be reached quantifying the effect of the R-substituents on the pK$_a$ values. From the mid-1930's the primary means to assess the effect of a substituent in the meta or para position of the benzene ring have been the Hammett σ constants (Hammett, 1937). The σ constants were originally formulated from the logarithm of the ratios of the acid-dissociation constants of substituted benzoic acids relative to the acid-dissociation constant of benzoic acid itself. Since the definition of σ considers a reference compound respect to it the effect of the substituent is measured, we hypothesize that for a same substituent, the σ constant value should be the same for benzoic acids and PSA acids, once we take the 6-H substituted PSA, (compound 1 in table 5) as reference structure to isolate the effect of the R substituent group.

The results of this comparison are shown in Table 6. It is possible to observe that the calculated σ values of this study for the selected substituents, not only, do exhibit the correct qualitative trend, but also show quantitative accuracy, within the error reported by Hammett. This finding validates the quality of the pK$_a$'s values calculated in this study.

In Fig. 5, the pK$_a$ values are plotted as function of σ for benzoic acids and PSA compounds with the same substituents. The figure shows a strong correlation between the pK$_a$'s and the

Compound	R	pK$_a$	Compound	R	pK$_a$
1	6-H	4.0	**21**	6-OCH(CH$_3$)$_2$	4.3
2	6-F	3.4	**22**	6-OC$_4$H$_9$	4.2
3	6-Cl	3.4	**23**	6-OCHF$_2$	3.8
4	5-F	3.7	**24**	6-OC$_6$H$_5$	4.0
5	5-Cl	3.6	**25**	5-OCH$_3$	3.8
6	3-F	3.9	**26**	5-OC$_6$H$_5$	3.9
7	5,6-(Cl)$_2$	3.3	**27**	6-SCH$_3$	4.1
8	6-C$_6$H$_5$	4.4	**28**	6-SC$_2$H$_5$	4.2
9	6-CH$_3$	4.0	**29**	6-SC$_3$H$_7$	4.2
10	6-C$_2$H$_5$	4.0	**30**	5-SCH$_3$	4.0
11	6-C$_3$H$_7$	4.0	**31**	6-CO$_2$CH$_3$	4.1
12	6-CF$_3$	3.5	**32**	6-COC$_6$H$_5$	4.2
13	5-CH$_3$	4.0	**33**	6-COCH$_3$	3.6
14	5-C$_2$H$_5$	4.0	**34**	6-NO$_2$	3.7
15	5-CN	3.4	**35**	6-CH$_3$SO$_2$	3.9
16	5-CCH	3.7	**36**	6-NH$_2$	4.3
17	3-CH$_3$	4.0	**37**	5-NH$_2$	3.7
18	6-OCH$_3$	4.3	**38**	5-NO$_2$	3.4
18	6-OC$_2$H$_5$	4.1	**39**	5-OH	3.8
20	6-OC$_3$H$_7$	4.2			

Table 5. Calculated acid-dissociation constants for R-substituted PSA compounds.

Substituent	Benzoic acids [42]		DMPS acids	
	pK$_a$	σ	pK$_a$	σ
m-chloro	3.83	0.37 ± 0.04	3.6	0.4
m-cyano	3.60	0.678	3.4	0.6
m-fluor	3.87	0.34 ± 0.08	3.7	0.3
m-hydroxy	4.08	0.12	3.8	0.2
m-methoxy	4.09	0.12 ± 0.12	3.8	0.2
m-methyl	4.27	-0.07 ± 0.04	4.0	0.0
m-nitro	3.49	0.71 ± 0.07	3.4	0.6

Table 6. pK$_a$'s and Hammet σ constants for selected substituents of benzoic acids and PSA compounds.
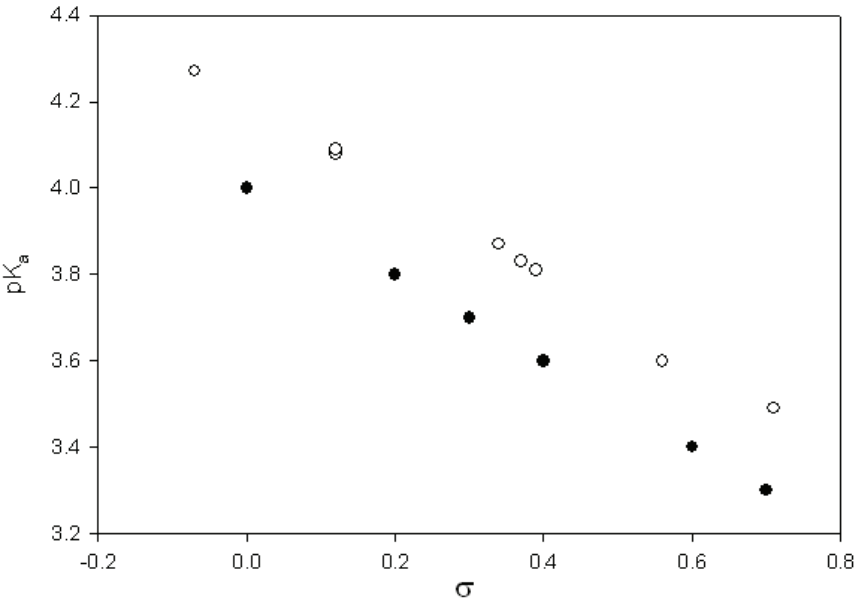
Fig. 5. pK$_a$ vs the Hammett σ constants (open circles: benzoic acids; solid circles: PSA compounds.

σ constants for the two families of compounds. Both straight lines are shifted in an extent that we identify as a consequence of the substituent effect of the ODMP group.

Additionally to the above checking procedure, we propose a second checking test in order to discard the presence of potential systematic errors in the method. The reported correlation equation of pK$_a$ as function of σ for benzoic acids is (Hollingsworth at al., 2002):

$$pK_a = 4.20 - \sigma \tag{3}$$

This equation allows us to predict the pK$_a$'s of the compounds of this study if we consider the ODMP group as a substituent of the respective benzoic acids, once the value of the Hammett σ constant for this group is known. This value can be determined by taking the logarithm of the ratios of the acid-dissociation constants of the R-substituted PSA compounds to the respective R-substituted benzoic acids shown in Table 6, in analogy to the

original definition of Hammett for σ for benzoic acids. This procedure allows to isolate the substituent effect of the ODMP group.

The results of these calculations are shown in Table 7; the resulting mean is 0.21. With this value of σ for the ODMP group and the respective value for the other substituent, we are able to predict the pK_a´s for the family of compounds of this study using the empirical equation (3) obtained for substituted benzoic acids. The predicted pK_a's coincide exactly with those values calculated in this study using DFT methodology, Figure 6.

Substituent	σODMP
6-H	0.189
5-F	0.169
5-Cl	0.228
5-CH$_3$	0.270
5-CN	0.200
5-OCH$_3$	0.288
5-NO$_2$	0.089
5-OH	0.278

Table 7. Hammett σ constants for the O-dimethoxypyrimidinyl group (ODMP)
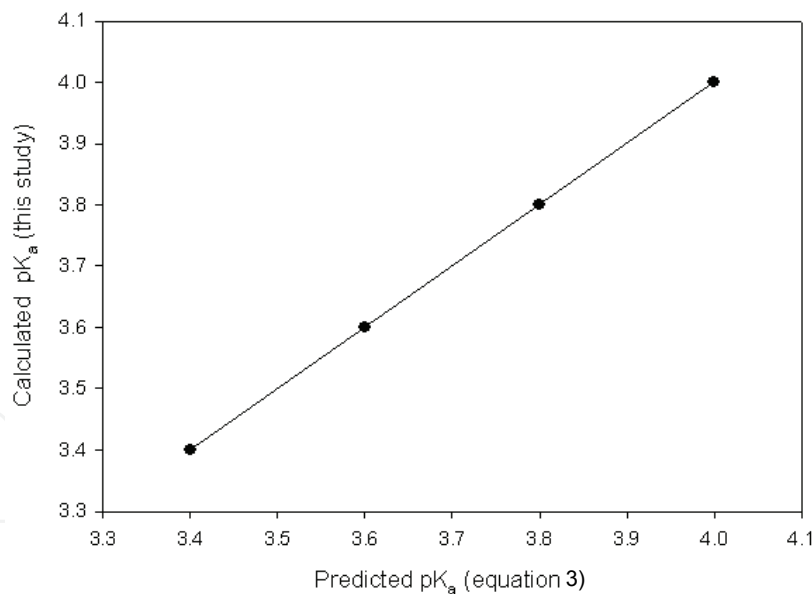
Fig. 6. Calculated pK_a (this study) vs. predicted pK_a (eqn. 3) for PSA compounds.

6.3 Theoretical calculation of partition coefficients pf PSA compounds

Continuing with the physicochemical characterization of this family of herbicides, we have reported environmentally important partition coefficients, Henry´s law constant, H, octanol/water, K_{OW}, and octanol/air, K_{OA}, partition coefficients for 39 PSA compounds (Delgado, 2010). These coefficients are calculated using density functional theory (DFT) at B3LYP/6-31G(d,p) level of theory using the Poisson-Boltzmann solvation model. These

properties have not been reported previously for this family of herbicides, neither experimentally nor theoretically.

6.3.1 Thermodynamics

Free energy of solvation ΔG_s^0, in addition to its fundamental interest, may combined with other thermodynamic data to predict a variety of equilibrium constants, being one of the most important the partitioning of a solute between two immiscible phases. Therefore, ΔG_s^0 is a key property to estimate the fate of a chemical once it is released in the environment. From an environmental point of view, three of the most important partition coefficients are the Henry´s law constant (H), the octanol/air (K_{OA}) and the octanol/water (K_{OW}) partition coefficients which can be calculated straightforwardly from the free energies of solvation in water and octanol by means of the well known equations:

$$\ln H = \ln(RT) + \Delta G_s^0(water) / RT \tag{4}$$

$$\log K_{OA} = -\Delta G_s^0(oct) / 2.303RT \tag{5}$$

$$\log K_{OW} = \left\{ \Delta G_s^0(water) - \Delta G_s^0(oct) \right\} / 2.303RT \tag{6}$$

6.3.2 Computational methods

Initial three-dimensional geometries of the chemical structures were generated using Hyperchem 7.0 molecular modeling package. These 3D structures were refined later using the Jaguar suite and its graphic interface Maestro. Gas-phase molecular geometries and electronic energies were obtained by density functional theory (DFT) calculations at the same level of theory, basis set including polarization functions on all atoms in conjunction with the hybrid functional B3LYP, which uses a combination of the three-parameter Becke exchange functional along with the Lee-Yang-Parr nonlocal correlation functionals: B3LYP/6-31G(d,p). To determine the lowest-energy conformation for each molecule, geometry optimizations were carried out allowing one or more torsional angles to vary systematically. Free energies of solvation in water and octanol were computed by single point calculations, including implicit solvation, on the gas-phase optimized geometry using the Poisson-Boltzmann Solvation Model (Marten et al., 1996).

6.3.3 Results

The calculated free energies of solvation in water and octanol, along with the respective values of the Henry´s law constants, the octanol/air partition and the octanol/water partition coefficients are shown in Table 8.

From this table it is possible to observe that all these compounds have low values of gas/solvent partition coefficients, consequently they show low volatility and a clear preference for the condensed phases. The preferred condensed phase, either water or octanol, is determined by the value of K_{OW}. The calculated values of log K_{OW} range from – 0.50 to about 3.0, breaking down in the following way: two cases, compounds 35 and 39, with negative values; three cases, compounds 24, 26 and 38, with values greater than 2; and the remaining compounds having intermediate values between 0 and 2.

	R	$\Delta G_S^0(water)$ $(kJ\,mol^{-1})$	$\Delta G_S^0(oc\tan ol)$ $(kJ\,mol^{-1})$	H (Pa m^3 mol^{-1})	K_{OA}	Log K_{OW}
1	6-H	-44.22	-49.20	4.44E-05	4.17E+08	0.87
2	6-F	-42.80	-48.79	7.88E-05	3.53E+08	1.05
3	6-Cl	-43.39	-47.82	6.21E-05	2.39E+08	0.78
4	5-F	-42.47	-48.20	9.00E-05	2.78E+08	1.00
5	5-Cl	-40.46	-46.74	2.02E-04	1.54E+08	1.10
6	3-F	-43.89	-48.41	5.08E-05	3.03E+08	0.79
7	5,6-(Cl)$_2$	-40.79	-46.11	1.77E-04	1.20E+08	0.93
8	6-C$_6$H$_5$	-49.75	-55.10	4.77E-06	4.51E+09	0.94
9	6-CH$_3$	-38.99	-45.69	3.66E-04	1.01E+08	1.17
10	6-C$_2$H$_5$	-40.25	-45.77	2.20E-04	1.05E+08	0.97
11	6-C$_3$H$_7$	-39.96	-45.35	2.48E-04	8.84E+07	0.94
12	6-CF$_3$	-42.09	-47.99	1.05E-04	2.56E+08	1.03
13	5-CH$_3$	-43.64	-48.33	5.61E-05	2.93E+08	0.82
14	5-C$_2$H$_5$	-42.30	-47.78	9.64E-05	2.35E+08	0.96
15	5-CN	-52.93	-64.22	1.32E-06	1.79E+11	1.98
16	5-CCH	-44.35	-53.76	4.22E-05	2.63E+09	1.65
17	3-CH$_3$	-44.89	-45.40	3.39E-05	8.99E+07	0.09
18	6-OCH$_3$	-43.43	-52.43	6.11E-05	1.53E+09	1.58
18	6-OC$_2$H$_5$	-42.89	-51.76	7.60E-05	1.17E+09	1.55
20	6-OC$_3$H$_7$	-42.47	-51.55	9.00E-05	1.07E+09	1.59
21	6-OCH(CH$_3$)$_2$	-48.74	-54.77	7.17E-06	3.94E+09	1.06
22	6-OC$_4$H$_9$	-41.63	-51.34	1.26E-04	9.87E+08	1.70
23	6-OCHF$_2$	-45.06	-55.23	3.17E-05	4.74E+09	1.78
24	6-OC$_6$H$_5$	-37.74	-54.35	6.07E-04	3.33E+09	2.91
25	5-OCH$_3$	-45.98	-54.81	2.18E-05	4.01E+09	1.55
26	5-OC$_6$H$_5$	-39.08	-56.74	3.53E-04	8.71E+09	3.09
27	6-SCH$_3$	-45.06	-50.12	3.17E-05	6.05E+08	0.89
28	6-SC$_2$H$_5$	-44.98	-50.58	3.27E-05	7.29E+08	0.98
29	6-SC$_3$H$_7$	-44.77	-50.25	3.56E-05	6.37E+08	0.96
30	5-SCH$_3$	-43.64	-48.33	5.61E-05	2.93E+08	0.82
31	6-CO$_2$CH$_3$	-52.26	-59.41	1.73E-06	2.57E+10	1.25
32	6-COC$_6$H$_5$	-55.31	-61.21	5.07E-07	5.30E+10	1.03
33	6-COCH$_3$	-55.61	-59.12	4.49E-07	2.28E+10	0.61
34	6-NO$_2$	-50.25	-61.42	3.90E-06	5.77E+10	1.96
35	6-CH$_3$SO$_2$	-76.36	-74.64	1.04E-10	1.20E+13	-0.30
36	6-NH$_2$	-53.76	-57.24	9.47E-07	1.07E+10	0.61
37	5-NH$_2$	-65.73	-66.32	7.58E-09	4.16E+11	0.10
38	5-NO$_2$	-48.41	-61.04	8.20E-06	4.96E+10	2.21
39	5-OH	-69.50	-66.40	1.66E-09	4.30E+11	-0.54

Table 8. Calculated free energy of solvation in water and octanol, Henry´s law constant, octanol-air partition coefficient and octanol-water partition coefficient for R-substituted O-pyrimidinylsalicylic acids.

Those with negative values show preference for the aqueous phase. This behavior is explained, in the case of compound 35, by the high polar nature of the sulfonyl group which provides an highly hydrophilic character. Moreover, it is well known that sulfones are able to stabilize negative charges on neighbor atoms, such as those of the carboxylic group. On the other hand, in the compound 39, the hydroxyl group in meta position with respect to the carboxylic group strengthens the acidity by inductive effect, favoring in consequence its water solubility.

On the other hand, those compounds with values of log K_{OW} > 2 will have preference for the octanol phase. This behavior is explained in terms of the high hydrophobic character provided by the OC_6H5 and NO_2 substituent groups present in compounds 24, 26 and 38. This finding is in agreement with the empirical evidence of the surprisingly low solubility in water of these compounds, therefore in the ambient they will be preferably found in the lipids of aquatic and animal biota and potentially they could scale in the food chain.

6.3.4 Discussion

The validation of the calculated figures unfortunately can not be made in a direct way since for this family of compounds there is no experimental data available to check the calculated values. However, indirectly we can have an estimation of their reliability. For instance, a recent paper reports the following model, based on the fragmental method, to predict the log K_{OW} of halogenated benzoic acids in terms of certain group and factor values (Qiao et al., 2008):

$$\log K_{OW}^{HBz} = \sum_{i=1}^{11} n_i g_i + \sum_{j=1}^{2} l_j f_j + 1.117 \qquad (7)$$

where n_i is the number of i-type groups, g_i is the value of the group i, l_j is the number of j-type factors, f_1 and f_2 denote the factors for *ortho* and *para* substituents, respectively. The model reproduces the experimental data of log K_{OW} for halogenated benzoic acids with an average absolute error of 0.22 log units. Since, the DMPS-compounds of our study can be viewed as benzoic acids substituted in the ortho position with a O-dimethoxypyrimidynil (ODMP) group, we hypothesize this model should be also valid to our compounds. If it is so, we could apply the model to determine the group value for the ODMP group using our calculated values of log K_{OW} and the group and factor values reported by Qiao for the analog R-substituted benzoic acids. The results of these calculations are shown in Table 9; the resulting mean is –0.768. If this value for the ODMP group is correct, we should be able to reproduce the experimental values of log K_{OW} for R-substituted benzoic acids from the calculated log K_{OW} for the analog R-substituted PSA compound, since structurally benzoic acids can be viewed as DMPS acids without the ODMP group; therefore the application of eqn. (7) leads to the following equation:

$$\log K_{OW}^{HBz} = \log K_{OW}^{PSA} - g_{ODMP} - f_2 - \Delta g \qquad (8)$$

where g_{ODMP} is the value for the ODMP group, f_2 is the factor value for ortho substituents, and Δg accounts for the difference in the group value of the benzene ring with two and three substituents. The results of these calculations are shown in Table 10. The average absolute error of log K_{OW} is 0.26, quite comparable with the reported error (0.22) for the original data set of halogenated benzoic acids. This result allows to confirm the quality of the values of

K_{OW} calculated in this study, and also it validates the applicability of eqn. (7) for this family of compounds.

Substituent	ODMP group value
6-H	-0.679
6-F	-0.260
6-Cl	-1.039
5-F	-0.726
5-Cl	-1.135

Table 9. Group values for the *O*-dimethoxypyrimidinyl group (ODMP).

Compound	Exp. log K_{OW} (Qiao et al., 2008)	Calc. log K_{OW} (eqn. 8)
Benzoic acid	1.87	2.06
o-chlorobenzoic acid	2.05	1.87
m-chlorobenzoic acid	2.68	2.19
o-fluorobenzoic acid	1.77	2.14
m-fluorobenzoic acid	2.15	2.09

Table 10. Experimental and calculated log K_{OW} for benzoic acids.

The value of the Henry´s law constant is determined fundamentally by the free energy of solvation in water according to eqn. (4). The reliability of the methodology used in this article to calculate ΔG_S^0 in water was confirmed in an earlier article (Delgado, 2010), and consequently the values of H derived from it.

Since the calculated values of K_{OW} and H are supported by the above checking procedures, then the calculated values of K_{OA} should be also checked considering that these three coefficients are related by the well known equation (Meylan & Howard, 2005):

$$K_{OA} = RT \frac{K_{OW}}{H} \tag{9}$$

Thus, the plot of K_{OA}, calculated according to eqn. (5), vs (K_{OW} / H) should give rise to a straight line whose slope equals to RT. The plot, shown in Figure 7, confirm this fact and therefore supports the calculated values of K_{OA}. Moreover, the value of the slope corresponds to the value of RT at 298 K, within the error of the methodology.

7. Concluding remarks.

Modern chemistry is oriented more and more towards the elucidation in detail of how the macroscopic properties are determined by the microscopic properties of matter, this current tendency is motivated by both academic and applied reasons. From academic point of view, it allows to have a detailed picture of the intermolecular interactions that determine the macro properties; and from an applied point of view, it allows systematize the search of a compound with desired properties in base of its molecular structure, selecting, in this way, the most promising compounds to be synthesized on a rational base. Quantum chemical
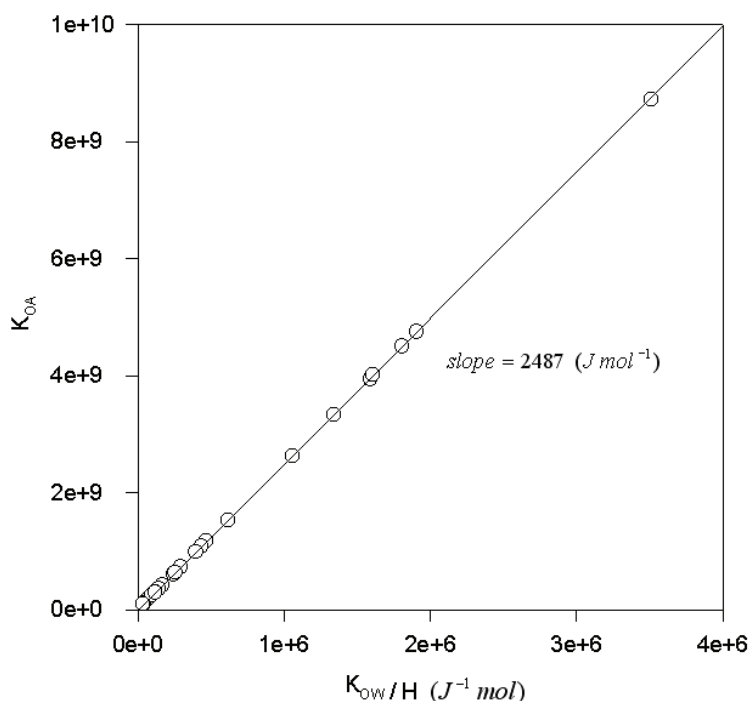
Fig. 7. Calculated K_{OA} (eqn. 2) vs (K_{OW} /H)

calculations allow the most accurate description of the electronic and geometric structure of molecules, as well as their interactions. These methods, which range from semi-empirical to *ab initio* approaches, have advantages and drawbacks which are necessary to evaluate before their use, since there exists a compromise among accuracy, computation time, physical interpretation and applicability.

Several computer-assisted quantum chemical approaches have been successfully applied to a variety of chemical systems, ranging their applicability from biological chemistry (Lie & Schiott, 2008) to chemical engineering (Sandler, 1999, 2003), passing by pesticide (Wan et al., 2004) and environmental chemistry (Delgado & Alderete, 2002). Thus, theoretical studies often may be considered not only as other option, but also as the only option in those cases in which the empirical information is not ready available, like those showed in this chapter.

In closing, we believe that computer-assisted quantum chemical studies represent one of the most important approaches in the present and future of chemistry, since they, on one hand, allow to obtain information not available from other techniques, and, on the other hand, the phenomena can be understood at molecular level, this is essential for the design of novel herbicides since their properties may be predicted prior to synthesis and consequently the design may, in this way, be guided by the results of calculations.

8. Acknowledgement.

9. References

Ballschmiter, K. (1992). Transport and fate of organic compounds in the global environment. *Angew. Chem. Int. Ed. Engl.* 31, 487-515.

Cramer, C.J. (2002). *Essentials of Computational Chemistry. Theories and Models*, John Wiley & Sons Ltd., Chichester.

Cramer, R.D.; Patterson, D.E.; Bunce, J.D. (1988). Comparative molecular field analysis (CoMFA). 1. Effect of shape on binding of steroids to carrier proteins. *J. Am. Chem. Soc.* 110, 5959-5967.

Delgado, E.J. (2009). DFT calculation of pK$_a$`s for dimethoxypyrimidinylsalicylic based herbicides. *Chem. Phys. Lett.* 471, 133-135.

Delgado, E.J. (2010). Theoretical calculation of partition coefficients of dimethoxypyrimidinylsalicylic Acids. *J. Mol. Model.* (in press), DOI 10.1007.

Delgado, E.J; Alderete, J. (2002). On the calculation of Henry´s law constants of chlorinated benzenes in water from semiempirical quantum chemical methods. *J. Chem. Inf. Comput. Sci.* 42, 559-563.

Diaz, G.A.; Delgado, E.J. (2009). Quantitative prediction of AHAS inhibition by pyrimidinylsalicylate based herbicides. *Pestic. Biochem. Physiol.* 95, 33-37.

Duffy, E.M.; Jorgensen, W.L. (2000). Prediction of properties from simulations: free energies of solvation in hexadecane, octanol and water. *J. Am. Chem. Soc.*, 122, 2878-2888.

Duggleby, R.G.; Pang, S-S. (2000). Acetohydroxyacid synthase. *J. Biochem. Mol. Biol.* 33, 1-36.

Estrada, E.; Delgado, E.J.; Alderete, J.B.; Jaña, G.A. (2004). Quantum-connectivity descriptors in modeling solubility of environmentally important organic compounds. *J. Comput. Chem.* 25, 1787-1796.

Estrada, E.; Delgado, E.J.; Simon-Manso, Y. (2007). Modeling the solubility in water of environmentally important organic compounds, In: *Thermodynamics, Solubility and Environmental Issues*, Trevor L. Letcher, (Ed.), 17-29, Elsevier, Amsterdam.

Frenkel, D.; Smit, B. (1996). *Understanding Molecular Simulation*, Academic Press, San Diego, CA.

Hansch, C. (1993). Quantitative structure–activity relationships and the unnamed science. *Acc. Chem. Res.* 26, 147-153.

Hansch, C.; Hoekman, D.; Gao, H. (1996). Comparative QSAR: toward a deeper understanding of chemicobiological interactions. *Chem. Rev.* 96, 1045-1075.

Hammett, L.P. (1937). The effect of structure upon the reactions of organic compounds. Benzene derivates. *J. Am. Chem. Soc.* 59, 96.

He, Y.Z.; Li, Y.X.; Zhu, X.L.; Xi, Z.; Niu, C.; Wan, J.; Zhang, L.; Yang, G.F. (2007). Rational design on bioactive conformation analysis of pyrimidinylbenzoates as acetohydroxyacid symthase inhibitors by integrating molecular docking, CoMFA, CoMSIA, and DFT calculations. *J. Comput. Chem.* 47, 2335-2344.

Hollingsworth, C.A.; Seybold, P.G.; Hadad, C.M. (2002). Substituent effects on the electronic structure and pK$_a$ of benzoic acid. *Int. J. Quantum. Chem.* 90, 1396-1403.

Karelson, M.; Lobanov, V.S.; Katritzky, A.R. (1996). Quantum-Chemical descriptors in QSAR/QSPR studies. *Chem. Rev.* 96, 1027-1043.

Katritzky, A.L.; Karelson, M.; Lobanov, V.S. (1997). QSPR as a means of predicting and understanding chemical and physical properties in terms of structure. *Pure & Appl. Chem.* 69, 245-248.

Klebe, G.; Abraham, U.; Mietzner, T. (1994). Molecular similarity indices in a comparative analysis (CoMSIA) of drug molecules to correlate and predict their biological activity. *J. Med. Chem.* 37, 4130-4146.

Kollman, P. (1993). Free-energy calculations – applications to chemical and biochemical phenomena. *Chem. Rev.* 93, 2395- 2417.

Lie, M.A.; Schiott, B. (2008). A DFT study of solvation effects on the tautomeric equilibrium and catalytic ylide generation of thiamin models. *J. Comput. Chem.* 29, 1037-1047.

Lyman Ott, R.; Longnecker, M. (2001). *An Introduction to Statistical Methods and Data Analysis*, Duxbury, Pacific Grove.

Marten, B.; Kim, K.; Cortis, C.; Friesner, R.A; Murphy, R.B.; Ringnalda, M.N.; Sitkoff, D.; Honig, B. (1996). New model for calculation of solvation free energies: correction of self-consistent reaction field continuum dielectric theory for short-range hydrogen-bonding effects. *J. Phys. Chem.* 100, 11775-11788.

Meylan, W.M., Howard, P.H. (2005). Estimating octanol-air partition coefficients with octanol-water partition coefficients and Henry´s law constants. *Chemosphere* 61,640-644.

McCourt, J.A.; Pang, S.S.; Guddat, L.W.; Duggleby, R.G. (2005). Elucidating the specifity of binding of sulfonylurea herbicides to Acetohydroxyacid synthase. *Biochemistry* 44, 2330-2338.

McCourt, J.A.; Duggleby, R.G. (2006). Acetohydroxyacid synthase and its role in the biosynthetic pathway for branched-chain amino acids. *Amino Acids* 31, 173-210.

McCourt, J.A.; Pang, S.S.; King-Scott, J.; Guddat, L.W.; Duggleby, R.G.(2006). Herbicide-binding sites revealed in the structure of plant Acetohydroxyacid synthase. *Proc. Natl. Acad. Sci. U.S.A.* 103, 569-573.

Nezu, Y.; Miyasaki, M.; Sugiyama, K.; Wada, N.; Kajiwara, I.; Miyazawa, T. (1996). Dimethoxypyrimidines as novel herbicides. Part 2.Synthesis and herbicidal activity of O-Pyrimidinylsalicylates and analogues. Pest. Sci. 47, 115-124.

Nezu, Y.; Wada, N.; Yoshida, F.; Miyazawa, T.;. Shimizu, T.; Fujita, T. (1998). Dimethoxypyrimidines as novel herbicides. Part 4. Quantitative structure-activity relationships of dimethoxypyrimidinyl(thio)salicylic acids. *Pestic. Sci.* 52, 343.-353

Pang, S.S.; Duggleby, R.G.; Guddat, L.W. (2002). Crystal structure of yeast Acetohydroxyacid synthase: a target for herbicidal inhibitors. *J. Mol. Biol.* 317, 249-262.

Pang, S.S.; Guddat, L.W.; Duggleby, R.G. (2003). Molecular basis of sulfonylurea herbicide inhibition of Acetohydroxyacid synthase. *J. Biol. Chem.* 278, 7639-7644.

Pang, S.S.; Duggleby, R.G.; Schowen, R.L.; Guddat, L.W. (2004). The crystal structures of *Klebsiella pneumoniae* acetolactate synthase with enzyme-bound cofactor and with an unusual intermediate. *J. Biol. Chem.* 279, 2242-2253.

Qiao, Y., Xia, S., Ma, P. (2008). Octanol/water partition coefficienrs of substituted benzene derivates containing halogens and carboxyls: determiantion using the shake-flask method and estimation using the fragment method. *J. Chem. Eng. Data* 53, 280-282.

Sandler, S.I. (1999). Unusual chemical thermodynamics. *J. Chem. Theromodynamics* 31, 3-25.

Sandler, S.I. (2003). Quantum Mechanics: a new tool for engineering thermodynamics, *Fluid Phase Equilibria* 210, 147-160.

Siepmann, J.I. (1999). Monte Carlo methods for simulating phase equilibria of complex fluids. *Adv. Chem Phys.* 105, 443-460.

Singh, B. K.; Shaner, D.L. (1995). Biosynthesis of branched chain amino acids: from test tube to field. *Plant Cell* 7, 935-944.

Stangroom, S.J.; Lester, J.N.; Collins, C.D. (2000). Abiotic behaviour of organic micropollutants in soils and the aquatic environment. A review: I. Partitioming. *Environ. Technol*. 21, 845-863.

Stanton, D.T.; Jurs, P.C. (1990). Development and use of charged partial surface area structural descriptors in computer-assisted quantitative structure-property relationship studies. *Anal. Chem.* 62, 2323- 2329.

Tomasi, J.; Persico, M. (1994). Molecular interactions in solution: an overview of methods based on continuous distributions of the solvent. *Chem. Rev*. 94, 2027-2094.

Wan, J.; Zhang, L.; Yang, G. (2004). Quantitative structure-activity relationships for phenyl triazolinones of protoporphyrinogen oxidase inhibitors: a density functional theory study. *J. Comput. Chem.* 25, 1827-1832.

Wang, J.G.; Li, Z.M.; Ma, N.; Wang, B.L.; Jiang, L.; Pang, S.S.; Lee, Y.T.; Guddat, L.W.; Duggleby, R.G. (2005). Structure-activity relationships for a new family of sulfonylurea herbicides. *J. Comput. Aid. Mol. Des.* 19, 801-820.

Young, D. (2001). *Computational Chemistry. A practical guide for applying techniques to real world problems*, John Wiley & Sons, Inc., New York.

Zohar, Y.; Einav, M.; Chipman, D.M.; Barak, Z. (2003). Acetohydroxyacid synthase from Mycobacterium avium and its inhibition by sulfonylureas and imidazolines. *Biochim. Biophys. Acta* 1649, 97-105.

Herbicides and Environment

Edited by Dr Andreas Kortekamp

Herbicides are much more than just weed killers. They may exhibit beneficial or adverse effects on other organisms. Given their toxicological, environmental but also agricultural relevance, herbicides are an interesting field of activity not only for scientists working in the field of agriculture. It seems that the investigation of herbicide-induced effects on weeds, crop plants, ecosystems, microorganisms, and higher organism requires a multidisciplinary approach. Some important aspects regarding the multisided impacts of herbicides on the living world are highlighted in this book. I am sure that the readers will find a lot of helpful information, even if they are only slightly interested in the topic.

How to reference

In order to correctly reference this scholarly work, feel free to copy and paste the following:

INTECH
open science | open minds